Technical Note

Effect of Contrast Media on Single-Shot Echo Planar Imaging: Implications for Abdominal Diffusion Imaging

Vikas Gulani, MD, PhD,[1,2]* Jonathan M. Willatt, MD,[3] Martin Blaimer, PhD,[1,2,4] Hero K. Hussain, MD,[3] Jeffrey L. Duerk, PhD,[1,2] and Mark A. Griswold, PhD[1,2]

Purpose: The goal of this study was to determine the effect of contrast media on the signal behavior of single-shot echo planar imaging (ssEPI) used for abdominal diffusion imaging.

Materials and Methods: The signal of an ssEPI spin echo sequence in a water phantom with varying concentrations of gadolinium was modeled with Bloch equations and the predicted behavior validated on a phantom at 1.5T. Six volunteers were given gadolinium contrast and signal intensity (SI) time courses for regions of interest (ROIs) in the liver, pancreas, spleen, renal cortex, and medulla were analyzed. Student's *t*-test was used to compare precontrast SI to 0, 1, 4, 5, 10, and 13 minutes following contrast.

Results: The results show that following contrast ssEPI SI goes through a nadir, recovering differently for each organ. Maximal contrast-related signal losses relative to precontrast signal are 20%, 20%, 53%, and 67% for the liver, pancreas, renal cortex, and medulla, respectively. The SIs remain statistically below the precontrast values for 5, 4, and 1 minute for the pancreas, liver, and spleen, and for all times measured for the renal cortex and medulla.

Conclusion: Abdominal diffusion imaging should be performed prior to contrast due to adverse effects on the signal in ssEPI.

Key Words: abdomen; diffusion; MRI; EPI; contrast; gadolinium; kidneys; pancreas; liver; spleen
J. Magn. Reson. Imaging 2009;30:1203–1208.

DIFFUSION-WEIGHTED IMAGING (DWI) is a long-established technique for evaluation of the neurological system, but is relatively new in body imaging. It has, however, quickly become an important tool in the evaluation of abdominal pathology and function in the liver (1–4), pancreas (5–7), and kidneys (8–10). Applications include (but are not limited to) liver tumor detection and characterization of small lesions, evaluation and quantitation of hepatic fibrosis, diagnosis and characterization of solid and cystic pancreatic masses, evaluation of pancreatic exocrine function, evaluation of renal parenchymal disorders, and characterization of renal masses (1–10). An open clinical question is whether abdominal diffusion images should be acquired prior to or following contrast administration. The effect of contrast material could conceivably have positive, negative, or neutral effects on lesion conspicuity and detection, based on the various competing effects of contrast on signal intensity. Given the time pressure on the modern scanner schedule, it would be ideal to fit diffusion imaging into the present imaging protocols without expending additional table time. The typical abdominal imaging protocol consists of precontrast imaging, followed by multiple timed postcontrast series imaged at 20–180 seconds postcontrast, and then delayed imaging at 4–6 minutes postcontrast and in some cases 10–15 minutes postcontrast (for example, in the evaluation of cholangiocarcinoma). Thus, there is a window of ≈1–3 minutes between the 3- and 4–6-minute postcontrast scans which could potentially be used for diffusion imaging. There are published studies in the literature stating that the signal intensity (SI) and measured apparent diffusion coefficient (ADC, a quantitative measure of the diffusivity) in the brain are not affected by administration of contrast (11–13) and that the same is true in the liver (14).

[1]Department of Radiology, University Hospitals of Cleveland, Case Western Reserve University, Cleveland, Ohio, USA.
[2]Case Center for Imaging Research, University Hospitals of Cleveland, Case Western Reserve University, Cleveland, Ohio, USA.
[3]Department of Radiology, University of Michigan, Ann Arbor, Michigan, USA.
[4]Research Center for Magnetic Resonance Bavaria e. V, Würzburg, Germany.
Contract grant sponsor: National Institutes of Health (NIH); Contract grant numbers: 1KL2RR024990 (to V.G.), NIH 1R21DK073649-01A2 (to H.K.H.); Contract grant sponsor: Siemens Medical Solutions (to J.L.D., M.A.G.).
*Address reprint requests to: V.G., Department of Radiology, Case Western Reserve University, University Hospitals of Cleveland, Bolwell B120, 11100 Euclid Ave., Cleveland, OH 44106-8062.
E-mail: vikas.gulani@uhhospitals.org
Received March 7, 2009; Accepted August 11, 2009.
DOI 10.1002/jmri.21945
Published online in Wiley InterScience (www.interscience.wiley.com).

The anecdotal experience of the authors, however, has been to the contrary: DWI of the abdomen obtained for clinical purposes appeared to be of higher quality if obtained before, rather than after, contrast. This hypothesis, however, must be proven with data.

Gadolinium contrast agents are utilized primarily for their T_1 shortening effects, but it is well known that these agents also cause T_2 shortening (15). The two properties have opposite consequences—T_1 shortening causes an increase in SI, particularly on T_1-weighted images, while T_2 or T_2* shortening causes a decrease in SI. The latter effect can dominate at high gadolinium concentrations, a phenomenon that is seen, for example, in the bladder when gadolinium concentrates there after contrast excretion. The two effects are expected to also have opposing effects on lesion detectability—the improved signal-to-noise ratio (SNR) caused by T_1 shortening will improve the available signal for additional diffusion weighting and also likely improve lesion detection, while the T_2 shortening will degrade the signal, causing opposing effects on image quality, lesion detectability, and ADC quantification. Thus, the purpose of this study was to quantitatively evaluate the effect of gadolinium administration on the quality of DWI. It was hypothesized that T_2 shortening provided by circulating contrast media significantly decreases the SNR in the heavily T_2-weighted, single-shot echo planar imaging (ssEPI), leading to image degradation. This hypothesis was tested with theoretical calculation and experimental verification of predicted SI in a simple spin echo EPI experiment on a gadolinium phantom of varying concentrations and time-course experiments on human volunteers.

MATERIALS AND METHODS

Model/Phantom Experiment

The expected relaxation rates R_1 and R_2 in a saturation recovery experiment in the presence of various concentrations of contrast agent were modeled by the well-accepted relationships (16):

$$R_1(C) = 1/T_{1,0} + \alpha_1 C \quad (1)$$

$$\text{and } R_2(C) = 1/T_{2,0} + \alpha_2 C, \quad (2)$$

where C is the concentration, $T_{1,0}$ and $T_{2,0}$ are the published intrinsic T_1 and T_2 values without contrast (6), and the longitudinal and transverse relaxivities α_1 and α_2 were obtained experimentally from measurements on gadolinium solutions. An expected signal versus concentration curve for water was generated from simple Bloch equations assuming TR/TE of 2400/71 msec. Imaging was performed on a 1.5T Siemens Espree (Siemens Medical Solutions, Erlangen, Germany). All data analysis was performed offline in MatLab (MathWorks, Natick, MA). The predicted behavior for water was tested on spin echo EPI on a phantom with gadolinium solutions of various concentrations ranging from 0–5 mM (imaging performed with a 12-channel body array coil, ssSE-EPI, TR/TE = 2400/71 msec, parallel imaging factor 2, 38 cm field of view [FOV], 150 × 150 matrix [MX], 5 mm slice thickness).

Volunteer Study

The study was performed under a protocol approved by the Institutional Review Board (IRB) and is HIPAA-compliant. Informed written consent was obtained from all participants. Asymptomatic volunteers with no known renal dysfunction were administered gadolinium contrast (n = 6, gadoversetamide, Optimark, Mallinkrodt, St. Louis, MO; 0.1 mmol/mL, 0.1 mmol/kg up to maximum volume of 20 mL, 2 cc/sec followed by a 20-mL saline push), and serial ssSE-EPI images were obtained every minute (TR/TE 2400/71 msec, 36–38 cm FOV, 162 × 162 matrix, 5 mm slice thickness, b = 0 and 500 s/mm^2). SI was measured in 0.2 cm^2 ROIs in the renal cortex and medulla, liver, pancreas, and spleen from the b = 0 images, at two timepoints prior to contrast, and then at 13 timepoints separated by 1 minute each, beginning immediately following contrast and ending at 13 minutes postinjection. A total of 15 timepoints were thus measured. In the case of the kidneys, SI time courses were measured for the renal cortex and medulla bilaterally. Since MRI SI is in arbitrary units and can vary widely across subjects, the measured SI at each timepoint was normalized for each subject and each organ by dividing the SI by the mean initial SI over the two measurements at 1 and 2 minutes prior to contrast administration. The mean SI at each timepoint was also calculated and plotted for each organ over the individual subject time courses. The error on the mean SI was plotted as the standard deviation (SD) on the mean at each timepoint. An overall mean time course with error bars was plotted for each organ to compare the SI behaviors of the organs. SNR measurements were not used because with multicoil, parallel imaging data, noise is not uniform across the image and SNR measurements are not accurate. However, since noise is expected to be relatively stable over the timescale of these experiments, measuring a signal change in an ROI over time should be directly proportional to underlying changes in SNR.

For each organ the normalized mean SI prior to contrast was compared to the intensity immediately postcontrast, and 1, 4, 5, 10, and 13 minutes following contrast, using a two-tailed paired Student's t-test to analyze statistical differences in SI.

RESULTS

The predicted SIs for a simple spin-echo experiment for water in the presence of various gadolinium concentrations and the measured SI on a phantom are shown in Fig. 1 in blue and green, with the measured intensities tracking with the theoretically predicted values.

Normalized signal time course data from volunteers for the liver, pancreas, spleen, renal cortex, and renal medulla are shown in Figs. 2–6. Each individual time

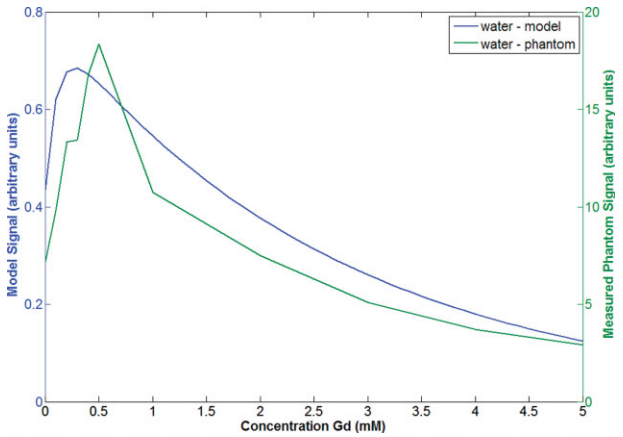

Figure 1. Simulation (blue) and measured phantom (green) SI for the predicted and actual behavior of a single-shot spin-echo EPI sequence at different gadolinium concentrations. [Color figure can be viewed in the online issue, which is available at www.interscience.wiley.com.]

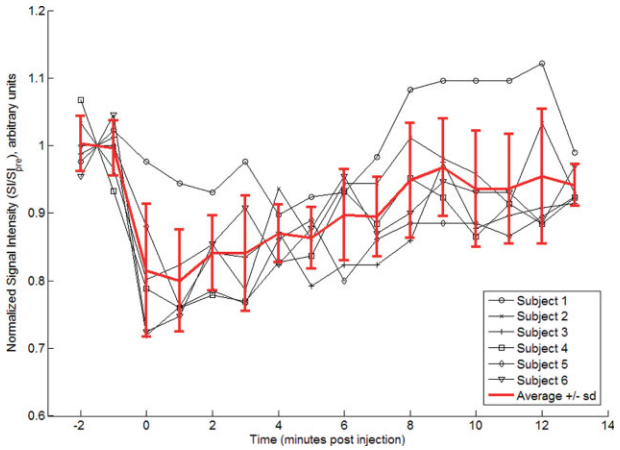

Figure 3. Individual time course and average (thick red line) normalized SI (SI/SI_{ave}) in the pancreas. Error bars for the average SI are calculated as the SD on the mean for each timepoint. [Color figure can be viewed in the online issue, which is available at www.interscience.wiley.com.]

course from a given subject is plotted with a different symbol and connected by corresponding lines, and the average time course (average ± SD) is shown as a thick solid red line. For the renal cortex and renal medulla, the time courses for the right side in each subject are plotted as described above, while the time courses on the left side are connected by a dashed line. The average time course is plotted as for the other organs. The average time course for each organ/region is also plotted in Fig. 7, to summarize these data and allow comparison between different organs. Finally, Fig. 8 depicts images of the right kidney at 0, 1, 2, and 5 minutes postcontrast administration, illustrating the effect of contrast on ssEPI of the kidneys. Note the severe degradation of the image quality in the b = 0/500 s/mm^2 images in Fig. 8g,h.

Table 1 summarizes normalized signal intensities prior to contrast (−1 minute), immediately postcontrast (0 minute), and at 1, 4, 5, 10, and 13 minutes postcontrast. The two-tailed paired Student's *t*-test comparisons between the precontrast ($t = -1$ minute) and the postcontrast timepoints above are given in parenthesis within the same table. Comparisons reaching statistical significance ($P < 0.05$) are shown in bold.

DISCUSSION

As can be seen from Fig. 1, at very low gadolinium concentrations water SI is expected to increase, but then decrease as gadolinium concentration increases. The measured phantom data (green) follow the predicted trend, although at higher contrast agent concentrations measured SIs are slightly lower than the model. This may relate to variations in contrast agent concentration, and also to the fact that the model we employ is simplistic, using only pure T_1 and T_2 effects in the Bloch equations, and not taking into account

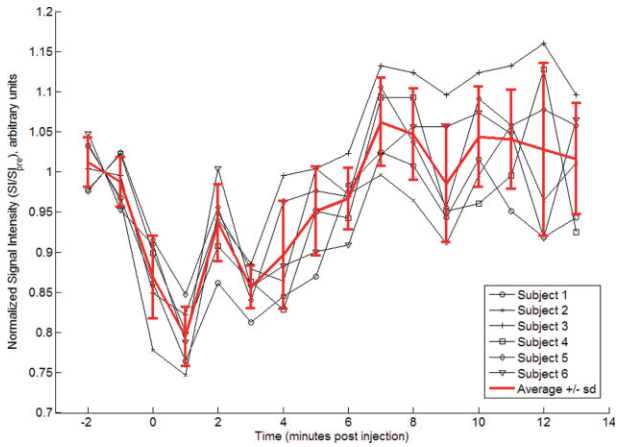

Figure 2. Individual time course and average (thick red line) normalized SI (SI/SI_{ave}) in the liver. Error bars for the average SI are calculated as the SD on the mean for each timepoint. [Color figure can be viewed in the online issue, which is available at www.interscience.wiley.com.]

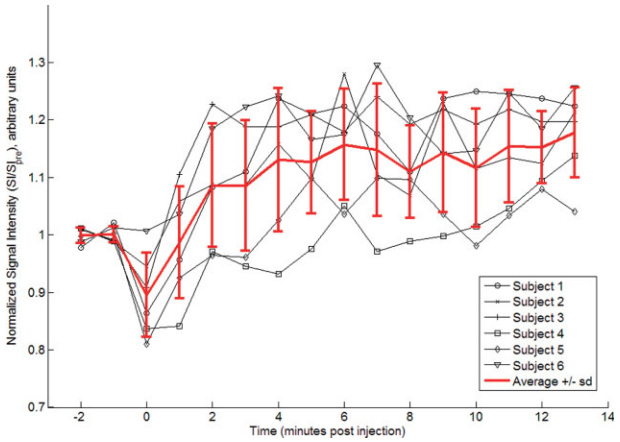

Figure 4. Individual time course and average (thick red line) normalized SI (SI/SI_{ave}) in the spleen. Error bars for the average SI are calculated as the SD on the mean for each timepoint. [Color figure can be viewed in the online issue, which is available at www.interscience.wiley.com.]

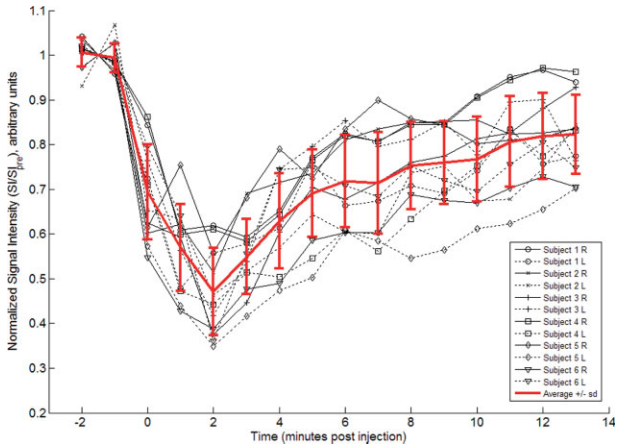

Figure 5. Individual time course and average (thick red line) normalized SI (SI/SI_{ave}) in the renal cortex. Error bars for the average SI are calculated as the SD on the mean for each timepoint. For each subject, data for the right and left kidneys are plotted as solid and dotted lines, respectively.

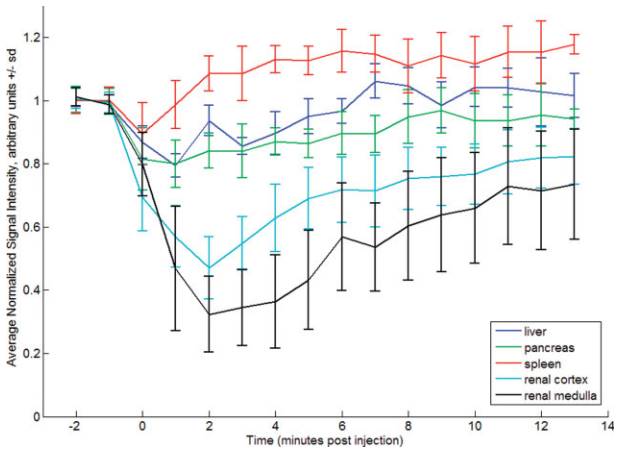

Figure 7. Normalized SI (SI/SI_{ave}) time courses in the liver, pancreas, spleen, renal cortex, and renal medulla.

other mechanisms of signal loss such as off-resonance distortions or relaxation during RF pulses. The important point, however, is that at higher concentrations of contrast agent the signal loss caused by T_2 decay outweighs the enhancement effect of the agent. Since adding diffusion weighting causes a significant net loss of signal, the goal is generally to preserve as much signal as possible so that there is sufficient signal to allow acquisition of higher b-value DWI, and improve lesion detection and characterization. At higher concentrations of gadolinium, this experiment clearly shows that the baseline SI for EPI would be nonideal (ie, nonmaximal) for DWI.

The volunteer time course data show reproducible signal behavior in EPI images of the liver, pancreas, spleen, and renal cortex and medulla (Figs. 2–7, numerical comparisons in Table 1). These organs/regions were chosen because these are the major areas of interest in the upper abdomen, and DWI of the regions must be performed with these regions in mind. There is a statistically significant drop in signal in all organs after injection of contrast. With the exception of the spleen, in which there is a recovery of signal within 2 minutes, it takes several minutes for the signal in the remaining organs to return to statistical baseline (presumably the T_1 shortening effects of the contrast agent dominate in the spleen). An additional observation about signal behavior in the liver is

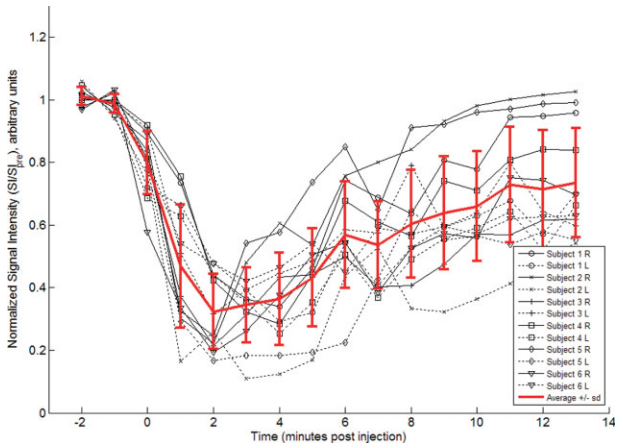

Figure 6. Individual time course and average (thick red line) normalized SI (SI/SI_{ave}) in the renal medulla. Error bars for the average SI are calculated as the SD on the mean for each timepoint. For each subject, data for the right and left kidneys are plotted as solid and dotted lines, respectively.

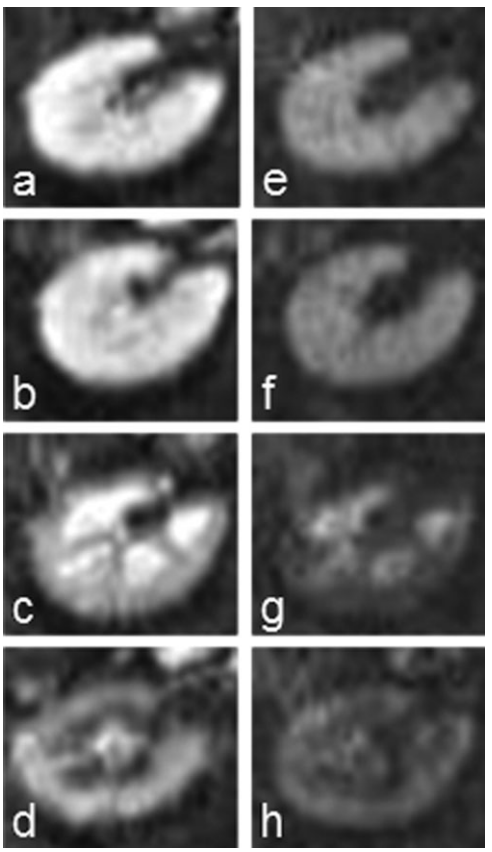

Figure 8. Single-shot EPI images cropped from a single time course to show the kidneys with b = 0 **(a–d)** and b = 500 s/mm^2 **(e–h)**, at times 0 (a,e), 1 minute (b,f), 2 minutes (c,g), and 5 minutes (d,h) postcontrast administration.

Table 1
Change in Normalized Signal Intensities Over Time

Time postcontrast (minutes)	Liver	Pancreas	Spleen	Renal cortex	Renal medulla
−1	0.99	1.00	1.00	0.99	0.98
0	**0.87 (0.002)**	**0.82 (0.01)**	**0.90 (0.01)**	**0.69 (0.000002)**	**0.82 (0.0001)**
1	**0.80 (0.00001)**	**0.80 (0.002)**	0.99 (0.68)	**0.57 (0.00000001)**	**0.47 (0.000002)**
4	**0.90 (0.02)**	**0.87 (0.004)**	1.13 (0.11)	**0.63 (0.0000002)**	**0.35 (0.00000002)**
5	0.95 (0.14)	**0.86 (0.001)**	**1.13 (0.04)**	**0.69 (0.000001)**	**0.41 (0.0000001)**
10	1.04 (0.11)	0.94 (0.12)	1.12 (0.08)	**0.77 (0.00002)**	**0.68 (0.0001)**
13	1.02 (0.41)	**0.94 (0.01)**	**1.18 (0.01)**	**0.82 (0.0001)**	**0.75 (0.0005)**

Mean normalized signal intensity (SI/SIave) in the liver, pancreas, spleen, renal cortex, and renal medulla prior to (−1 min) contrast, and at 0 minute, 1 minute, 4 minutes, 5 minutes, 10 minutes, and 13 minutes following contrast. *P* values from two−tailed paired Student's *t*−test comparing normalized signal intensities for each organ/region at times prior to contrast (−1 min) with normalized signal intensities at 0 minute, 1 minute 4 minutes, 5 minutes, 10 minutes, and 13 minutes following contrast are given in parentheses. Comparisons reaching statistical significance are shown in bold ($P < 0.05$).

that there is a second sharp decrease in SI between 2 and 3 minutes after contrast. This drop (≈8%) is also found to be significant ($P = 0.005$) and may relate to arrival and concentration of contrast from the portal circulation, although this hypothesis would require further experimental testing.

There is actually a reversal of cortex/medulla contrast in the kidney roughly 2 minutes after injection (Figs. 5–8). Importantly, for the liver, pancreas, renal cortex, and medulla there are contrast-related signal losses of 20%, 20%, 53%, and 67%, respectively, all of which are statistically significant. The signal is measured to be statistically below baseline for the first 4 minutes for liver, first 8 minutes and at 13 minutes for pancreas (signal measurements and *t*-test calculations for minutes 6–8 are not shown in Table 1), and beyond 13 minutes for either renal cortex or medulla. These results confirm the preliminary observations on a single subject published in abstract form previously (17). The results for these organs indicate that if images are obtained after contrast injection there would be loss of valuable signal, a key problem for an already SNR-starved technique such as DWI, which relies on further signal *loss* to achieve the desired image contrast and quantification. Moreover, since dynamic contrast-enhanced images are typically obtained at 20–180 seconds after contrast, if the DWI were to be performed postcontrast, images would be most likely obtained 4–6 minutes after injection, the signal nadir for the kidneys and pancreas, and a time at which liver signal is also low. This means that the DWI would be performed at the most suboptimal time if the organ of interest is any of these three. Even if diffusion imaging is performed more than 10 minutes postinjection of contrast, the situation is suboptimal for evaluating the kidneys, pushing forward a strong argument that diffusion weighting should not be performed in the postcontrast set of sequences in the abdomen and doing so could negatively affect the diagnostic performance of the sequence. The drop in signal could result in low SI lesions to drop to noise level, rendering them undetectable, and could adversely affect the conspicuity of other lesions. Quantitation of ADC in lesions and surrounding parenchyma will be adversely affected because less signal will be available to obtain higher diffusion weighting, and also quantitation of the ADC is less accurate with noisier data.

The observed behavior is different from that reported in the literature on the brain, where it has been shown that the presence of gadolinium contrast has little effect on DWI (11–13). This difference likely relates to a higher concentration of contrast agent in abdominal organs (particularly the kidney), and the absence of a blood–brain barrier in the abdomen. Also, the dynamic nature of enhancement in the abdomen has a clear effect on the signal behavior in the abdomen after contrast administration. The most likely explanation for the difference between these results and those reported for the liver previously, which suggested that there is no difference in the SNR of liver DWI obtained before and after contrast, is that the single timepoint used for postcontrast imaging in the previous study is long enough postcontrast that the liver signal had recovered to baseline or near baseline (14). Also, the previous study was performed at 3.0T and the present study was at 1.5T. Relaxation properties due to contrast agent are different at high fields, and thus time course SIs could differ as well.

As long as the DWI is performed at a time where the signal behavior of the sequence is not dynamically changing, one would not expect the ADC to change significantly due to the presence of contrast. These experiments show (Figs. 2–7 and Table 1), however, that dynamically changing signal behavior would be nearly impossible to avoid after contrast, particularly in the kidneys. The adverse effect of data noise on the accuracy of calculated diffusion coefficients in both isotropic and anisotropic diffusion was not evaluated here, but has been previously well documented (18–20).

As mentioned previously, lesion characterization and ADC quantification, especially tumor detection and characterization in the liver, pancreas, and kidneys are critical reasons to perform diffusion imaging in the abdomen. Therefore, an important additional consideration is the effect of contrast on tumors. The dynamics of contrast behavior in tumors and the effects on EPI are not predictable, and indeed likely vary from tumor to tumor. In the liver, for example, the contrast-related alteration in ssEPI signal behavior may be drastically different for an arterially

perfused tumor such as hepatocellular carcinoma than for a relatively poorly perfused mass such as cholangiocarcinoma. It is not possible to say a priori whether a given tumor will behave like the renal cortex/medulla in which the SI is adversely affected 13 minutes or more beyond the administration of contrast, or more like the spleen, where there may even be an increase in baseline signal due to contrast. If for a given mass at a given timepoint there is a contrast-related signal loss sufficient to drop the higher b value SI to noise levels, then the measured ADC would also be affected (the calculated ADC can be predicted to be lower than the actual value due to the SI hitting a noise floor and not changing due to increased diffusion weighting). This unpredictable behavior is another reason to avoid diffusion imaging in the abdomen after contrast.

In conclusion, this work shows that in planning whether to place the diffusion sequences for the abdomen before or after contrast, the effect of the contrast on the EPI SI should be taken into account, and assuming normal physiology, the DWI should be performed before contrast. If the decision is made to place the diffusion imaging after contrast, a minimum of 6 minutes postcontrast should be allowed when normal circulation is expected, in which case the effect of changing signal behavior in the ssEPI sequences generally employed will likely preclude accurate characterization of the kidneys.

REFERENCES

1. Koinuma M, Ohashi I, Hanafusa K, Shibuya H. Apparent diffusion coefficient measurements with diffusion-weighted magnetic resonance imaging for evaluation of hepatic fibrosis. J Magn Reson Imaging 2005;22:80–85.
2. Naganawa S, Sato C, Nakamura T, et al. Diffusion-weighted images of the liver: comparison of tumor detection before and after contrast enhancement with superparamagnetic iron oxide. J Magn Reson Imaging 2005;21:836–840.
3. Quan XY, Sun XJ, Yu ZJ, Tang M. Evaluation of diffusion weighted imaging of magnetic resonance imaging in small focal hepatic lesions: a quantitative study in 56 cases. Hepatobiliary Pancreat Dis Int 2005;4:406–409.
4. Sun XJ, Quan XY, Huang FH, Xu YK. Quantitative evaluation of diffusion-weighted magnetic resonance imaging of focal hepatic lesions. World J Gastroenterol 2005;11:6535–6537.
5. Inan N, Arslan A, Akansel G, et al. Diffusion-weighted imaging in the differential diagnosis of cystic lesions of the pancreas. Am J Roentgenol 2008;191:1115–1121.
6. Lee SS, Byun JH, Park BJ, et al. Quantitative analysis of diffusion-weighted magnetic resonance imaging of the pancreas: usefulness in characterizing solid pancreatic masses. J Magn Reson Imaging 2008;28:928–936.
7. Erturk SM, Ichikawa T, Motosugi U, et al. Diffusion-weighted MR imaging in the evaluation of pancreatic exocrine function before and after secretin stimulation. Am J Gastroenterol 2006;101: 133–136.
8. Cova M, Squillaci E, Stacul F, et al. Diffusion-weighted MRI in the evaluation of renal lesions: preliminary results. Br J Radiol 2004;77:851–857.
9. Squillaci E, Manenti G, Cova M, et al. Correlation of diffusion-weighted MR imaging with cellularity of renal tumours. Anticancer Res 2004;24:4175–4179.
10. Thoeny HC, De Keyzer F, Oyen RH, Peeters RR. Diffusion-weighted MR imaging of kidneys in healthy volunteers and patients with parenchymal diseases: initial experience. Radiology 2005;235:911–917.
11. Yamada K, Kubota H, Kizu O, et al. Effect of intravenous gadolinium-DTPA on diffusion-weighted images: evaluation of normal brain and infarcts. Stroke 2002;33:1799–1802.
12. Fitzek C, Mentzel HJ, Fitzek S, et al. Echoplanar diffusion-weighted MRI with intravenous gadolinium-DTPA. Neuroradiology 2003;45:592–597.
13. Chen G, Jespersen SN, Pedersen M, et al. Intravenous administration of Gd-DTPA prior to DWI does not affect the apparent diffusion constant. Magn Reson Imaging 2005;23:685–689.
14. Chiu FY, Jao JC, Chen CY, et al. Effect of intravenous gadolinium-DTPA on diffusion-weighted magnetic resonance images for evaluation of focal hepatic lesions. J Comput Assist Tomogr 2005;29:176–180.
15. Caravan P, Ellison JJ, McMurry TJ, Lauffer RB. Gadolinium(III) chelates as MRI contrast agents: structure, dynamics, and applications. Chem Rev 1999;99:2293–2352.
16. Haacke EM, Brown RW, Thompson MR, Venkatesan R. Magnetic resonance imaging: physical principles and sequence design. New York: John Wiley & Sons; 1999.
17. Gulani V, Blaimer M, Nour SG, et al. Effect of contrast media on the signal intensity of single-shot EPI for diffusion imaging of the body. In: Proc 15th Annual Meeting ISMRM, Berlin; 2007:3833.
18. Pierpaoli C, Basser PJ. Toward a quantitative assessment of diffusion anisotropy. Magn Reson Med 1996;36:893–906.
19. Basser PJ, Pajevic S. Statistical artifacts in diffusion tensor MRI (DT-MRI) caused by background noise. Magn Reson Med 2000; 44:41–50.
20. Chen B, Hsu EW. Noise removal in magnetic resonance diffusion tensor imaging. Magn Reson Med 2005;54:393–401.